

ORIGINAL  
RESEARCH

F. Miese  
G. Kircheis  
H.J. Wittsack  
F. Wenserski  
J. Hemker  
U. Mödder  
D. Häussinger  
M. Cohnen

# <sup>1</sup>H-MR Spectroscopy, Magnetization Transfer, and Diffusion-Weighted Imaging in Alcoholic and Nonalcoholic Patients with Cirrhosis with Hepatic Encephalopathy

**PURPOSE:** Mild swelling of astrocytes is proposed as a key event in the pathogenesis of hepatic encephalopathy. Proton MR spectroscopy (<sup>1</sup>H-MR spectroscopy), diffusion-weighted imaging (DWI), and magnetization transfer imaging were performed in patients with alcoholic and nonalcoholic liver cirrhosis and correlated with different clinical stages of hepatic encephalopathy to assess alterations in cerebral water metabolism in different subgroups of patients with cirrhosis.

**MATERIAL AND METHODS:** Forty-five patients (26 alcoholics, 19 nonalcoholics [due to hepatitis C ( $n = 9$ ), hemochromatosis ( $n = 2$ ), primary chronic cholangitis ( $n = 2$ ), hepatitis B ( $n = 1$ ), Wilson disease ( $n = 1$ ), cryptogenic cirrhosis ( $n = 4$ )] and 18 controls underwent <sup>1</sup>H-MR spectroscopy, magnetization transfer imaging, and DWI of the basal ganglia and normally appearing occipital white matter (NAWM). *N*-acetylaspartate (NAA), choline (Cho), myo-inositol (mIns), and glutamine/glutamate (Glx) relative to creatine (Cr), the apparent diffusion coefficients (ADC), and the magnetization transfer ratios (MTR) were correlated to the neuropsychologic status, which was assessed by computerized psychometry and mental state grading, according to the West Haven criteria.

**RESULTS:** Compared with controls, nonalcoholic subjects exhibited a gradual increase of Glx/Cr in the basal ganglia and NAWM; a decrease in mIns/Cr; a significant decrease of MTR in the thalamus, the putamen, the pallidum, and NAWM; and an increase in the ADC of the NAWM with increasing hepatic encephalopathy severity. In alcoholics, mIns/Cr of the basal ganglia and the NAWM, Cho/Cr of the basal ganglia, and MTR of all assessed regions were decreased. Glx/Cr of the basal ganglia and of the NAWM was increased, compared with that of controls; but no correlation to the clinical hepatic encephalopathy grading was found. ADC did not change significantly between the groups.

**CONCLUSIONS:** Apart from a typical pattern of <sup>1</sup>H-MR spectroscopy alterations in hepatic encephalopathy, a gradual decrease in MTR and an increase of ADC was found correlating to clinical grading of hepatic encephalopathy in nonalcoholic patients with cirrhosis. In alcoholic patients with hepatic encephalopathy, there was no such correlation. Abnormalities detected by MR imaging may hint at different pathways of brain damage in alcohol-induced liver disease.

Mild swelling of astrocytes is proposed as a key event in the pathogenesis of hepatic encephalopathy.<sup>1</sup> Proton MR spectroscopy (<sup>1</sup>H-MR spectroscopy) studies in patients with liver cirrhosis almost uniformly show a decrease in the ratio of choline to creatine (Cho/Cr), a decrease in myo-inositol (mIns/Cr), and an elevation in cerebral glutamine and creatine (Glx/Cr) signal intensity.<sup>2-7</sup> Astrocytic glutamine accumulation due to ammonia, other neurotoxins, and oxidative/nitrosative stress with reactive depletion of the osmosensitive mIns and other osmolite pools is a widely accepted interpretation of these findings.<sup>8-10</sup> In the present study, <sup>1</sup>H-MR spectroscopy was performed to test whether the well-investigated spectroscopic alterations in hepatic encephalopathy can be found in both subgroups of patients with alcoholic and nonalcoholic subtypes of cirrhosis.

Magnetization transfer contrast imaging has shown a decrease of the magnetization transfer ratio (MTR) in normal-appearing white matter (NAWM) and normal-appearing gray

matter regions in patients with cirrhosis with manifest hepatic encephalopathy.<sup>11,12</sup> Reversibility after successful liver transplantation was interpreted as an indicator of increased free cerebral water, thus supporting the hypothesis of mild astrocyte swelling as a major pathogenetic event in hepatic encephalopathy.<sup>13</sup> We performed magnetization transfer imaging in both subgroups of patients with cirrhosis to test whether alterations of magnetization transfer are present in alcoholic as well as in nonalcoholic patients with cirrhosis.

The first study using diffusion-weighted imaging (DWI) in hepatic encephalopathy showed an increase of the apparent diffusion coefficient (ADC) in NAWM and in the basal ganglia except in the thalamus in nonalcoholic patients with cirrhosis, a finding reported to indicate an ammonia-induced increase in brain-water mobility and content.<sup>14</sup> In this article, ADC was determined as a means to differentiate intracellular and extracellular edema. A direct measurement of absolute brain-water content was not performed.

Although various imaging findings have been described in patients with alcoholic liver cirrhosis, to our knowledge, no data on magnetization transfer imaging and DWI have been published for this specific subgroup and the nonalcoholic subtype of cirrhosis. Furthermore, imaging findings in different degrees of hepatic encephalopathy defined by computer psychometry have not been analyzed previously. Therefore, this

Received June 22, 2005; accepted after revision September 20.

From the Institute of Diagnostic Radiology (F.M., H.J.W., F.W., U.M., M.C.), University Hospital Düsseldorf and the Department of Internal Medicine (G.K., J.H., D.H.), Division of Gastroenterology, Hepatology, and Infectious Diseases, University Hospital Düsseldorf, MNR Clinic, Moorenstr 5, 40225 Düsseldorf, Germany.

Please address correspondence to: M. Cohnen, MD, University Hospital Düsseldorf, Institute of Diagnostic Radiology, MNR Clinic, Moorenstr 5, 40225 Düsseldorf.

**Table 1: Patients and controls**

	Controls (n = 18)	Alcoholics (n = 26)	Nonalcoholics (n = 19)
(M/F) Sex	8/10	18/8	14/5
Age (±SD), y	55.7 ± 13.8	54.3 ± 12.7 NS	61.1 ± 12.4 NS
CFF (±SD), Hz	41.3 ± 1.6	37.3 ± 5.0**	36.6 ± 4.9**
Child-Pugh grading			
A		10	9
B		11	5
C		5	5
HE grading			
HE 0		7	5
mHE		8	3
HE 1		5	6
HE 2		6	5

**Note:**—Forty-five cirrhotics and 18 controls were enrolled. In 8 controls, 2 alcoholics, and one nonalcoholic patient magnetic resonance spectroscopy could not be performed. Values are reported as mean ± SD. HE indicates hepatic encephalopathy; mHE, minimal HE. \*\* Significantly different from controls  $P < .01$  (Mann-Whitney  $U$ ; NS indicates no significant difference).

investigation was performed to test whether  $^1\text{H}$ -MR spectroscopy, magnetization transfer imaging, and DWI can demonstrate alterations associated with increasing severity of hepatic encephalopathy and whether these alterations affect both white and gray matter. Furthermore, we investigated whether alterations can be found in both alcoholic and nonalcoholic patients with liver cirrhosis.

## Patients and Methods

**Characteristics of Subjects.** Forty-five patients with cirrhosis and 18 age-matched controls were included in the study (Table 1). All patients and volunteers gave written informed consent. Cirrhosis was due to alcohol abuse in 26 patients. Alcohol abuse was diagnosed clinically and on the basis of a history of a regular intake of more than 3 units of alcohol per day on a regular basis in the absence of another etiologic factor of liver cirrhosis, particular viral hepatitis. Other causes like hepatitis B or C, primary biliary cirrhosis, or a combination of them were found in 19 patients. The control group consisted of 8 men and 10 women; the alcohol-positive cirrhotic group, of 18 men and 8 women; and the alcohol-negative cirrhotic group, of 14 men and 5 women. All alcoholics were abstinent during the study phase. Subjects with a history of drug abuse with neurologic or psychiatric diseases were excluded from the study. In addition, patients treated with central nervous system (CNS)-relevant medications such as benzodiazepines, benzodiazepine antagonists, antidepressants, etc were excluded from the study. Severe disease such as spontaneous bacterial peritonitis, decompensated renal insufficiency, decompensated diabetes mellitus, or coronary heart diseases were further exclusion criteria. Patients with higher degrees of hepatic encephalopathy were excluded from the investigations, because asterixis, hyperreflexia, and other more severe stages such as stupor or somnolence did not allow safe and artifact-free MR imaging.

The severity of liver disease was determined according to the Child-Pugh score.<sup>15</sup> Alcoholics were graded Child-Pugh A in 10 patients, Child-Pugh B in 11 patients, Child-Pugh C in 5; nonalcoholics were graded Child-Pugh A in 9 patients, Child-Pugh B in 5, and Child-Pugh C in 5 (Table 1).

**Neuropsychologic Examination.** Five computer psychometric neurologic tests were performed on each patient. The test battery included the Visual Pursuit Test, Motor Performance Series, Cognitron, Vienna Reaction Test, and the Tachistoscopic Traffic Percep-

tion Test Mannheim for screen as part of the Vienna Test System.<sup>16</sup> Minimal hepatic encephalopathy was diagnosed if a patient showed no clinical overt symptoms of hepatic encephalopathy and performed  $<1$  standard deviation (SD) below the mean in at least 2 of the 5 computer psychometric tests of the test battery.<sup>17</sup> Other patients with cirrhosis without clinical overt hepatic encephalopathy performing below  $-1$  SD in only 1 of the tests were graded HE 0.<sup>17</sup> Overt encephalopathy was graded according to the West Haven criteria.<sup>18</sup> Alcoholics were graded HE 0 (no hepatic encephalopathy) in 7 patients, minimal hepatic encephalopathy (mHE) in 8 patients, HE 1 in 5 patients, and HE 1 in 6. Nonalcoholics were graded HE 0 in 5 patients, mHE in 3, HE 1 in 6, and HE 2 in 5 patients (Table 1).

**MR Imaging.** MR imaging was performed on a 1.5T clinical scanner (Magnetom Vision Plus, Siemens Medical Solutions, Erlangen, Germany) by using the standard head coil. Total examination time was approximately 40 minutes per subject.

**$^1\text{H}$ -MR Spectroscopy.** Single-voxel proton spectra were obtained from a volume of interest located in the white matter of the left occipital lobe and a second volume of interest located in the left basal ganglia, to assess both white matter and gray matter alterations. Volume size was a cube of  $20 \times 20 \times 20$  mm. Voxel size was kept constant for all examinations. Before recording the spectra, we optimized homogeneity of the magnetic field by shimming until a line width of the water signal intensity below 10 Hz was obtained. Water suppression was accomplished by using a frequency-selective prepulse on the water resonance. The spectra were obtained by using a single-volume spectroscopy-stimulated echo-acquisition method with short TE (TR/TE, 1500/20 ms; 128 acquisitions).

Spectrum analysis was performed off-line on an external workstation by means of the LCModel (version 5.2-2) and LCMgui (version 1.1-0) software (S.K. Provencher, Canada). The process of determining peak intensities of the different metabolites is described in detail elsewhere.<sup>19</sup> Relative concentrations of NAA, Glx, Cho, mIns, and the Cr resonance were used to calculate metabolite ratios with respect to the Cr resonance. In 8 controls, 2 alcoholics, and 1 nonalcoholic patient, lengthy imaging times were not tolerated and MR spectroscopy could not be performed.

**Magnetization Transfer Imaging.** Two 2D gradient-echo images were obtained (TR/TE, 700/12 ms;  $\alpha = 20^\circ$ ; 1 acquisition; 20 sections of 5-mm thickness; 0.5 mm gap), by using a matrix of  $224 \times 256$  pixels with a field of view of  $240 \times 240$  mm. The first was obtained before and the second after application of a saturation pulse 1.5 kHz below  $\text{H}_2\text{O}$  frequency with a bandwidth of 250 Hz, a 7.68-ms length, and a flip angle of  $500^\circ$ . The MTRs were quantified as a percentage of signal-intensity loss according to the following equation:

$$1) \quad \text{MTR} = (S_0 - S_s) / S_0 * 100\%,$$

where  $S_0$  is the mean signal intensity for a particular region obtained from the sequence without the saturation pulse and  $S_s$  is the mean signal intensity with the saturation pulse. The mean MTRs were determined in regions of interest manually drawn by 1 examiner (F.M.), placed in the thalamus, the globus pallidus, the putamen, the caudate head, occipital white matter (each reported as a mean of right and left), and the pons. Region-of-interest size was kept constant for all regions within 1 patient, with a minimum of 30 pixels not exceeding 300 pixels. Evaluation was performed by using a noncommercial software that automatically computes MTR pixel by pixel from the original imaging files. Gray values in these secondary images represent MTR data.

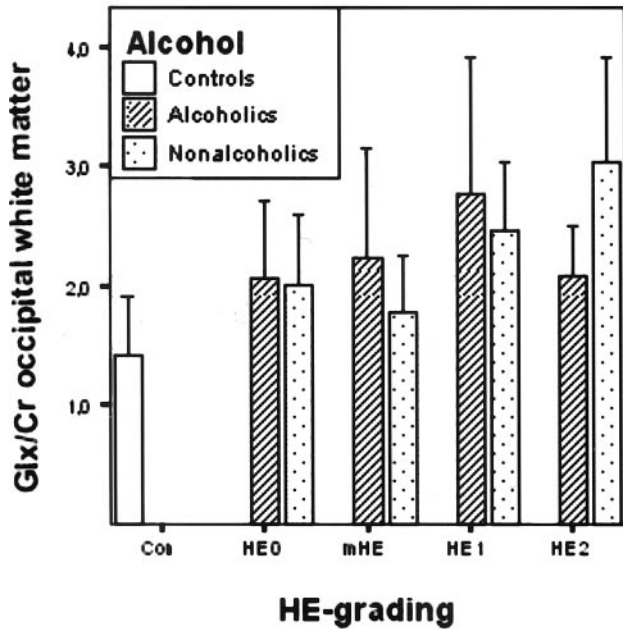


**Fig 1.** Graph shows hepatic encephalopathy grading and occipital white matter Glx/Cr in mean values; whiskers show SD. White matter Glx of alcoholics, graded mHE, HE 1, and HE 2 and white matter Glx of nonalcoholics with overt hepatic encephalopathy (HEO) are elevated, compared with that of controls (Co) ( $P < 0.05$ ; Mann-Whitney  $U$  test).

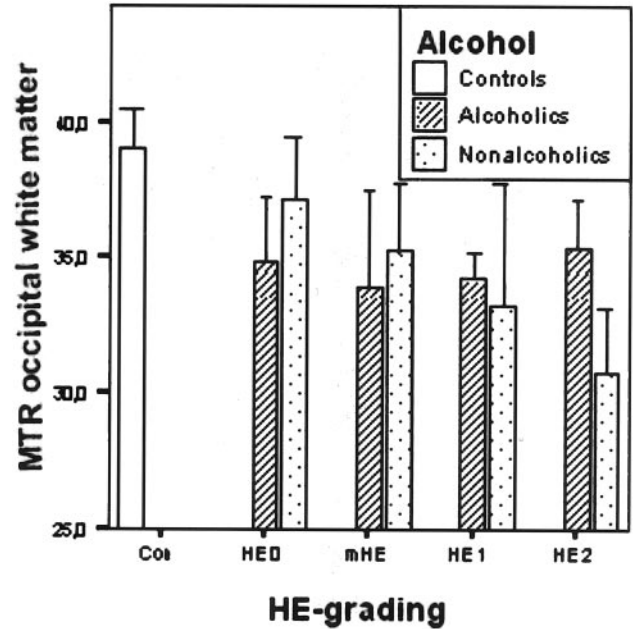


**Fig 2.** Graph shows hepatic encephalopathy-grading and occipital white matter MTR in mean values; whiskers show SD. White matter MTR of alcoholics, graded any hepatic encephalopathy, and white matter MTR of nonalcoholics with overt hepatic encephalopathy (HEO) are reduced, compared with that of controls (CO) ( $P < 0.05$ ; Mann-Whitney  $U$  test).

**DWI.** DWI was conducted by using single-shot spin-echo echo-planar imaging (TR/TE, 4000/100 ms; 1 acquisition; 20 sections of 5-mm thickness; 0.5-mm gap). The field of view was  $240 \times 240$  mm with a matrix of  $96 \times 128$  pixels. The diffusion-weighting gradients were applied on each of the 3 physical axes,  $x$ ,  $y$ , and  $z$ , in separate scans. Three different gradient strengths were chosen corresponding to b-factor values of 0, 500, and 1000 seconds/ $\text{mm}^2$ . Assuming a signal intensity attenuation depending monoexponentially on the b value, we determined the ADC of each direction pixelwise by using a least-squares fit according to the following equation:

$$2) \quad \text{ADC} = -1/b * \ln(S(b)/S_0).$$

By calculating the mean of the 3 directions, we generated the ADC trace map. The mean ADC was determined in manually drawn regions of interest placed in the thalamus, occipital white matter (reported as the mean of right and left), and the pons. Regions of interest were placed by 1 examiner (F.M.) and were positioned in identical areas for MTR and MR spectroscopy.

**Statistical Methods.** Statistical analysis was conducted by using SPSS software (version 10.1.3, Statistical Package for the Social Sciences, Chicago, Ill). Results of different groups were compared by using the nonparametric Mann-Whitney  $U$  test, assuming significance at a level of  $P < .05$ . Spearman rank correlation was used to calculate correlation coefficients.

## Results

**$^1\text{H-MR}$  Spectroscopy.** In the nonalcoholic group, mIns/Cr and Cho/Cr of the basal ganglia were significantly reduced, compared with those of the controls, whereas Glx/Cr was increased. mIns/Cr of the NAWM was significantly reduced, NAA/Cr was slightly increased, and Glx/Cr was strongly increased (Fig 1). Hepatic encephalopathy severity correlated negatively with the mIns/Cr in the basal ganglia ( $r = -0.56$ ;  $P < .016$ ; Spearman rank correlation) and in the NAWM ( $r = -0.53$ ;  $P < .024$ ; Spear-

man rank correlation). A positive correlation was found between Glx/Cr of the basal ganglia and the NAWM with hepatic encephalopathy severity and between the NAA/Cr of the white matter voxel and hepatic encephalopathy severity (Table 2).

In patients with alcoholic cirrhosis mIns/Cr and Cho/Cr of the basal ganglia were decreased significantly, compared with those of controls, whereas Glx/Cr was increased. Correspondingly, in these patients with cirrhosis, mIns/Cr of the white matter was decreased and Glx/Cr was increased significantly (Fig 1). NAA/Cr of the alcoholic subgroup was not significantly different from that of the controls. No correlation between hepatic encephalopathy severity and MR spectroscopy parameters was found in the alcoholic subgroup (Table 3).

**Magnetization Transfer Imaging.** In nonalcoholic patients with cirrhosis, MTR of the thalamus, pallidum, putamen, caudate nucleus, and occipital white matter was significantly reduced compared with that of controls. MTR of thalamus, pallidum, putamen, and occipital white matter was negatively correlated with the hepatic encephalopathy severity ( $r = -0.44$  up to  $-0.67$ ;  $P < .06$  up to  $.002$ ) (Table 2, Fig 2). In the alcoholic subgroup, the MTR of all regions assessed was significantly decreased compared with that of controls. There was no correlation with hepatic encephalopathy severity (Table 3, Fig 2).

**DWI.** ADC was not significantly altered but showed a tendency toward increased values in the thalamus and in NAWM in nonalcoholic patients with overt hepatic encephalopathy. Occipital white matter ADC was higher with increasing hepatic encephalopathy severity (Table 2). In the patients with alcoholic cirrhosis, the ADC of none of the regions examined was significantly different between alcoholic patients with cirrhosis and controls (Table 3).

**Other.** In the subgroup of patients with nonalcoholic cirrhosis, there was a negative correlation between MTR and Glx/Cr of the occipital NAWM ( $r = -0.68$ ;  $P < .01$ ; Spearman rank corre-

**Table 2: Nonalcoholics: rank correlations of <sup>1</sup>H-MRS, MTR, and ADC and grading of hepatic encephalopathy**

	Nonalcoholics, Mean (±SD)					Correlation (Spearman-Rho)	
	Controls, Mean (±SD) n = 10	HE 0 n = 5	mHE n = 3	HE1 n = 5	HE2 n = 5	r	P
<sup>1</sup> H-MRS, n = 28							
Basal ganglia							
mIns/Cr**	0.784 (0.570)	0.320** (0.161)	0.414 (0.154)	0.250** (0.186)	0.095** (0.097)	-.56	.016
NAA/Cr	1.670 (0.252)	1.742 (0.314)	1.704 (0.057)	1.447 (0.303)	1.726 (0.292)	-.11	.676
Cho/Cr**	0.267 (0.041)	0.226 (0.032)	0.261 (0.071)	0.206* (0.039)	0.190* (0.055)	-.31	.206
Glx/Cr*	1.513 (0.556)	1.823 (0.608)	1.794 (0.316)	2.133 (0.554)	2.945** (0.392)	<b>.62</b>	<b>.006</b>
Occipital lobe							
mIns/Cr**	0.823 (0.099)	0.464 (0.416)	0.481 (0.423)	0.349** (0.201)	0.063** (0.072)	<b>-.53</b>	<b>.024</b>
NAA/Cr*	1.708 (0.175)	1.760 (0.305)	1.781 (0.257)	1.939* (0.123)	2.110** (0.076)	<b>.63</b>	<b>.005</b>
Cho/Cr	0.258 (0.042)	0.244 (0.046)	0.259 (0.075)	0.200* (0.036)	0.228 (0.030)	-.21	.397
Glx/Cr**	1.413 (0.489)	1.998 (0.594)	1.774 (0.484)	2.458** (0.590)	3.035** (0.887)	<b>.52</b>	<b>.027</b>
MTR (%), n = 37	n = 18	n = 5	n = 3	n = 6	n = 5		
Pons	40.1 (1.5)	40.1 (3.2)	38.5 (0.9)	40.2 (2.9)	37.9 (4.8)	-.17	.480
Thalamus**	39.4 (0.9)	38.8 (1.3)	38.9 (1.4)	37.1** (2.5)	35.6** (1.3)	<b>-.64</b>	<b>.003</b>
Pallidum**	37.1 (1.6)	34.4 (6.0)	32.5 (6.2)	28.7** (6.0)	25.7** (2.5)	<b>-.58</b>	<b>.010</b>
Putamen**	35.9 (1.5)	34.5 (3.5)	33.1 (3.1)	30.3** (3.7)	28.9** (1.7)	<b>-.61</b>	<b>.006</b>
Caudate**	36.5 (2.2)	35.3 (3.9)	31.2* (3.3)	31.1** (4.4)	30.73** (1.8)	-.44	.062
Occipital lobe**	39.0 (1.5)	37.2 (2.3)	35.3 (3.4)	33.2* (4.5)	30.76** (2.4)	<b>-.67</b>	<b>.002</b>
ADC (10.5 mm <sup>2</sup> s), n = 37	n = 18	n = 5	n = 3	n = 6	n = 5		
Thalamus	81.8 (4.7)	78.8 (2.3)	84.1 (2.1)	82.81 (4.6)	83.8 (3.8)	.42	.070
Occipital NAWM	93.1 (15.7)	86.1 (4.0)	86.7 (6.9)	94.6 (12.0)	104.0 (20.3)	<b>.48</b>	<b>.035</b>

**Note:**—<sup>1</sup>H-MRS indicates proton magnetic resonance spectroscopy; MTR, magnetization transfer ratio; ADC, apparent diffusion coefficient; HE, hepatic encephalopathy; mHE, minimal HE; mIns, myoinositol; Cr, creatine and phosphocreatine; NAA, N-acetylaspartate; Cho, choline-containing.

Bold figures indicate significance ( $P < .05$ ).

\* Significantly different from control group ( $P < .05$ , Mann-Whitney  $U$ ).

\*\* Significantly different from control group ( $P < .01$ , Mann-Whitney  $U$ ).

**Table 3: Alcoholics: rank correlations of <sup>1</sup>H-MRS, MTR, and ADC and grading of hepatic encephalopathy**

	Alcoholics, Mean (±SD)					Correlation (Spearman-Rho)	
	Controls, Mean (±SD) n = 10	HE 0 n = 6	mHE n = 7	HE1 n = 5	HE2 n = 6	r	P
<sup>1</sup> H-MRS, n = 34							
Basal ganglia							
mIns/Cr**	0.784 (0.570)	0.256** (0.198)	0.260** (0.214)	0.347* (0.191)	0.296* (0.247)	.03	.889
NAA/Cr	1.670 (0.252)	1.623 (0.321)	1.453 (0.204)	1.645 (0.185)	1.559 (0.164)	.03	.896
Cho/Cr**	0.267 (0.041)	0.205** (0.032)	0.186** (0.041)	0.217 (0.053)	0.203* (0.049)	.01	.980
Glx/Cr*	1.513 (0.556)	2.079* (0.417)	2.795** (0.618)	2.597** (0.724)	2.516 (1.747)	.09	.669
Occipital lobe							
mIns/Cr**	0.823 (0.099)	0.295* (0.296)	0.272** (0.191)	0.310** (0.103)	0.252** (0.158)	.12	.567
NAA/Cr	1.708 (0.175)	1.920 (0.283)	1.877* (0.118)	1.807 (0.262)	1.914 (0.365)	-.11	.601
Cho/Cr	0.258 (0.042)	0.257 (0.056)	0.225 (0.055)	0.253 (0.044)	0.226 (0.036)	-.12	.572
Glx/Cr**	1.413 (0.489)	2.071 (0.643)	2.229** (0.919)	2.774** (1.150)	2.084* (0.412)	0.00	.988
MTR (%), n = 44	n = 18	n = 7	n = 8	n = 5	n = 6		
Pons	40.1 (1.5)	39.5 (0.5)	38.4* (1.5)	38.2 (2.6)	39.1 (2.4)	-.11	.600
Thalamus**	39.4 (0.9)	39.5* (0.5)	38.4* (1.5)	38.2** (2.6)	39.1** (2.4)	-.07	.730
Pallidum**	37.1 (1.6)	37.9** (1.6)	37.6** (2.0)	37.9** (0.7)	37.6** (1.6)	.01	.974
Putamen**	35.9 (1.5)	32.1** (3.8)	29.1** (5.6)	28.7** (2.7)	32.9** (1.7)	-.06	.774
Caudate**	36.5 (2.2)	33.1 (1.7)	31.0* (2.6)	32.3** (1.3)	32.4** (2.5)	-.18	.389
Occipital lobe**	39.0 (1.5)	34.3** (4.0)	32.8** (4.1)	31.6** (2.1)	32.8** (3.6)	.08	.707
ADC (10.5 mm <sup>2</sup> /s), n = 44	n = 18	n = 7	n = 8	n = 5	n = 6		
Thalamus	81.8 (4.7)	79.4 (4.1)	82.1 (5.1)	86.4* (2.6)	82.4 (7.1)	.31	.121
Occipital NAWM	93.1 (15.7)	91.9 (4.7)	86.7 (8.0)	100.2 (7.8)	93.6 (8.6)	.18	.378

**Note:**—<sup>1</sup>H-MRS indicates proton magnetic resonance spectroscopy; MTR, magnetization transfer ratio; ADC, apparent diffusion coefficient; HE, hepatic encephalopathy; mHE, minimal HE; mIns, myoinositol; Cr, creatine and phosphocreatine; NAA, N-acetylaspartate; Cho, choline-containing.

\* Significantly different from control group ( $P < .05$ , Mann-Whitney  $U$ ).

\*\* Significantly different from control group ( $P < .01$ , Mann-Whitney  $U$ ).

lation) (Fig 3). There was a positive correlation between MTR and mIns/Cr ratio of the white matter ( $r = 0.53$ ;  $P < .05$ ; Spearman rank correlation). Glx/Cr of the NAWM correlated negatively with mIns/Cr ( $r = -0.62$ ;  $P < .01$ ; Spearman rank correlation) (Fig 4). In the nonalcoholic patients with cirrhosis, a negative correlation was found between the MTR of the thal-

amus and the Glx/Cr of the basal ganglia ( $r = -0.61$ ;  $P < .01$ ; Spearman rank correlation). The MTR of the thalamus and the mIns/Cr ratio of the basal ganglia showed a positive correlation.

In the alcoholic patients with cirrhosis, there was no correlation between white matter MTR and any other white matter

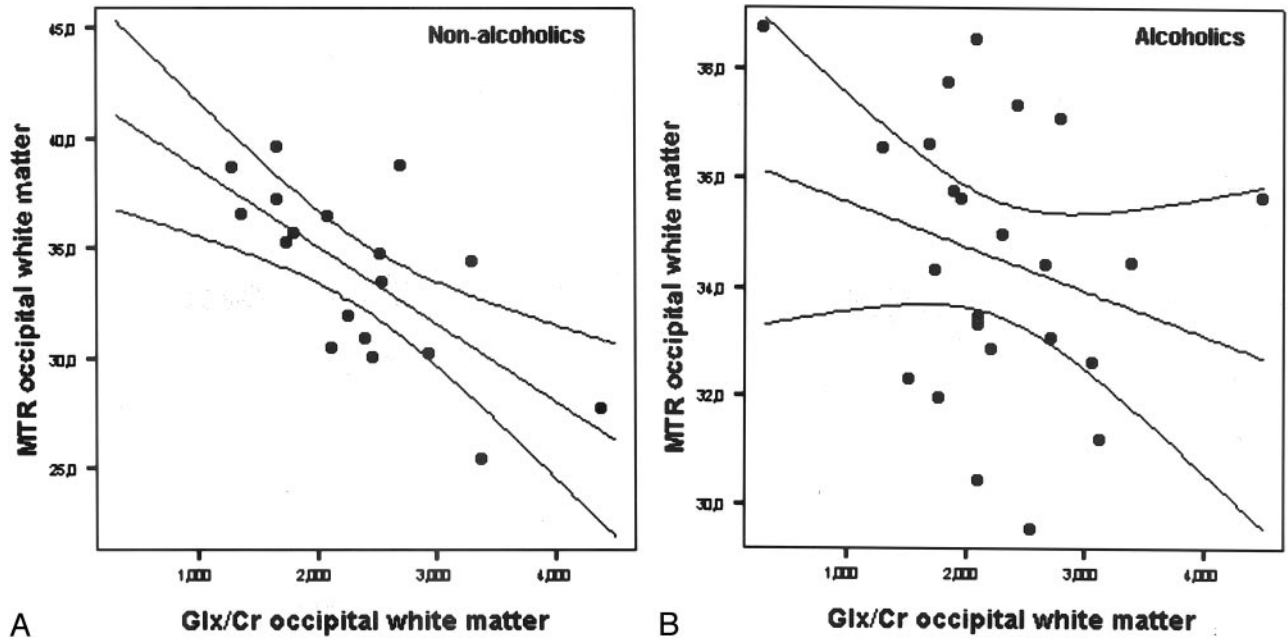


**Fig 3.** A, Nonalcoholics: occipital white matter Glx/Cr and MTR. Graph shows linear regression analysis ( $r^2=0.48$ ) and 95% predictive interval of means.  
 B, Alcoholics: occipital white matter Glx/Cr and MTR. Graph shows linear regression analysis ( $r^2 = 0.07$ ) and 95% predictive interval of means.

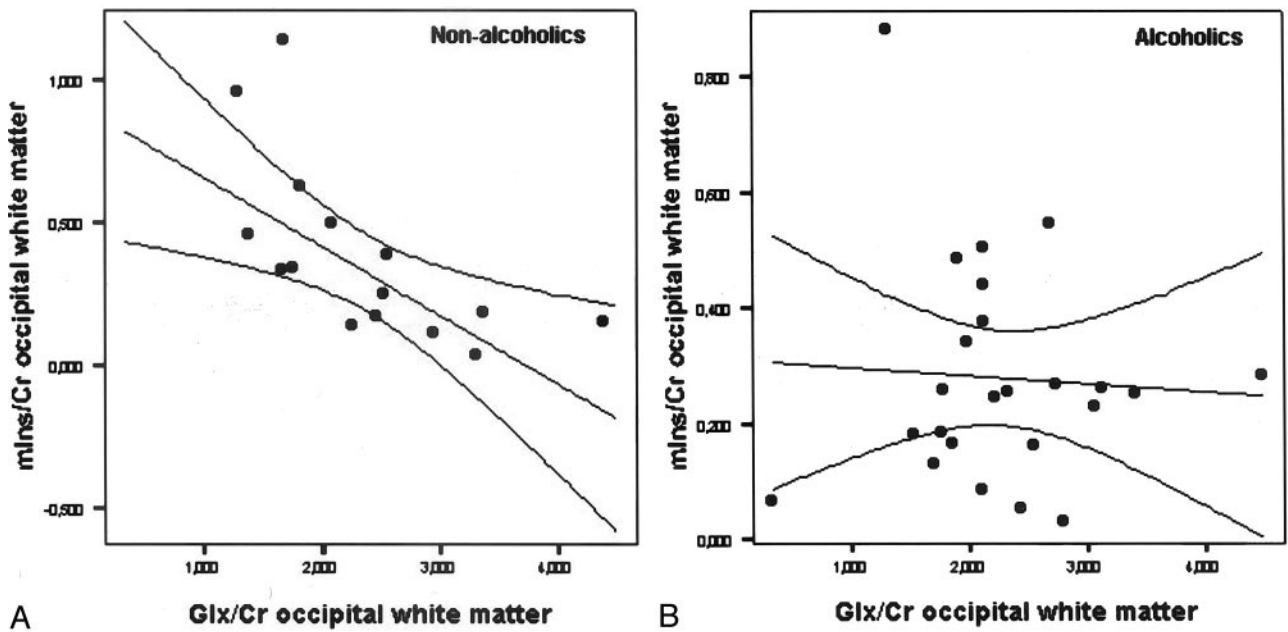


**Fig 4.** A, Nonalcoholics: occipital white matter Glx/Cr and mIns/Cr. Graph shows linear regression analysis ( $r^2 = 0.34$ ) and 95% predictive interval of means.  
 B, Alcoholics: occipital white matter Glx/Cr and mIns/Cr. Graph shows linear regression analysis ( $r^2=0.00$ ) and 95% predictive interval of means.

parameter. Also, no correlation between white matter Glx and mIns was found. In the basal ganglia, the MTR of the thalamus was weakly negatively correlated to the Glx/Cr ratio ( $r = -0.41$ ;  $P < .05$ ; Spearman-rank correlation). There was a negative correlation between NAA/Cr and Glx/Cr in the basal ganglia ( $r = -0.60$ ;  $P < .01$ ; Spearman rank correlation).

### Discussion

The present study reveals that in patients with liver cirrhosis, MTRs were decreased and ADCs were increased, compared with those of age-matched control subjects without neuropsychologic impairment.

Yet there are differences between alcoholic and nonalcoholic subjects.

Nonalcoholic patients with cirrhosis showed a pattern of MR imaging findings as previously reported. Briefly,  $^1\text{H-MR}$  spectroscopy revealed an increase in Glx/Cr and a decrease in the mIns/Cr and Cho/Cr ratio. This finding is considered typical in hepatic encephalopathy<sup>1</sup> and suggests that the subgroup of nonalcoholic patients with cirrhosis enrolled in the present study is comparable to groups of patients with cirrhosis studied previously.  $^1\text{H-MR}$  spectroscopy changes were similar in the basal ganglia and in the occipital white matter, pointing

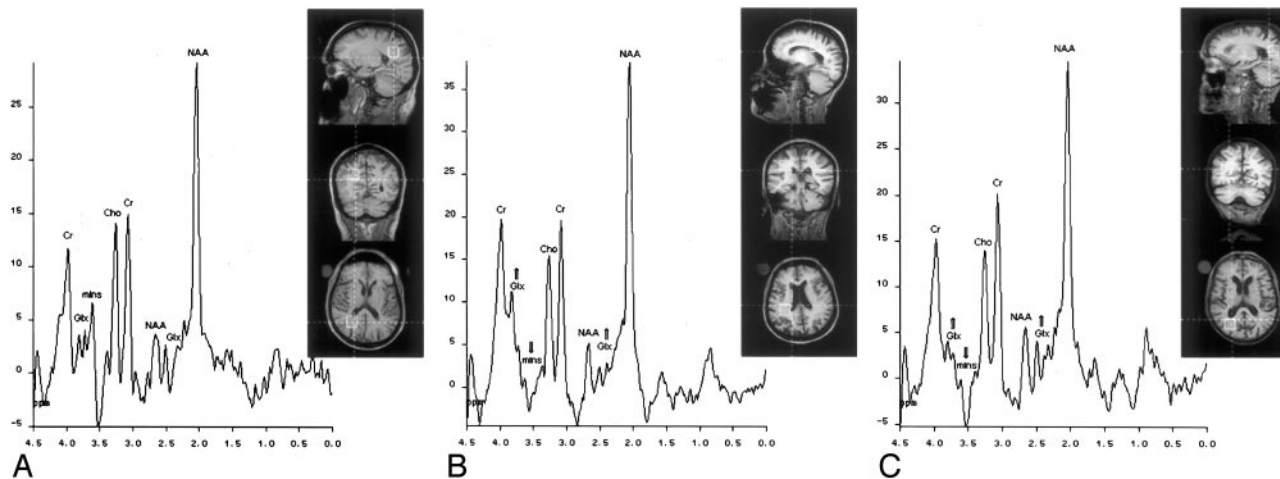


**Fig 5.** MR Spectra of posterior NAWM in a healthy control (A, patient 11), a nonalcoholic patient with cirrhosis (B, patient 55) with overt hepatic encephalopathy, and an alcoholic patient with cirrhosis (C, patient 59). Arrows indicate alterations in the patient's spectrum, compared with that of the control group. Control (A): mIns/Cr, 0.926; NAA/Cr, 1.952; Cho/Cr, 0.301; Glx/Cr, 1.442. Nonalcoholic patient with cirrhosis (B): mIns/Cr, 0.038; NAA/Cr, 2.129; Cho/Cr, 0.255; Glx/Cr, 3.307. Alcoholic patient with cirrhosis (C): mIns/Cr, 0.260; NAA/Cr, 1.722; Cho/Cr, 0.249; Glx/Cr, 1.784.

toward changes that affect gray and white matter in a similar manner. Therefore, effects of a systemic cause rather than local influences should be discussed.

Because these known changes are interpreted as possibly ammonia-induced, with an effect on osmoregulation and brain-water content, magnetization transfer imaging, which reflects changes in cerebral water content, was performed.<sup>11</sup> Corresponding to these previous results, the present study shows a decrease in the MTR of the basal ganglia and occipital NAWM in patients with cirrhosis. However, for the first time, a correlation of MR imaging findings with increasing severity of hepatic encephalopathy as defined by computer psychometry could be demonstrated. The MTR of the thalamus, globus pallidus, putamen, and white matter decreased significantly with increasing severity of hepatic encephalopathy in nonalcoholics. However, in contrast to nonalcoholic patients with cirrhosis, the marked decrease of MTR in alcoholic patients did not correlate with hepatic encephalopathy severity.

The decrease in the MTR may be explained by cellular loss and demyelination<sup>18-20</sup> or disturbance of brain-water content.<sup>11,21</sup> Rovira et al<sup>13</sup> demonstrated reversibility of MTR decrease in hepatic encephalopathy following successful liver transplantation, a finding unlikely in the case of axonal loss. The data of the present study indicate that there is neither a decrease of NAA/Cr in nonalcoholic patients nor a correlation between MTR and NAA/Cr, as should be expected in the case of structural alteration of white matter and loss of myelinated fibers. Furthermore, demyelinating lesions in progressive multifocal leukoencephalopathy have been reported to reduce MTR to half of the values found in the control group.<sup>22</sup> Compared with these results, the decrease of MTR in hepatic encephalopathy was very mild. Therefore, demyelination seems an unlikely explanation of MTR reduction found in patients with hepatic encephalopathy. A slight increase of brain-water content may, however, result in a relative rarefaction of magnetization transfer sites in relation to free water protons. A possible consequence may be a mild swelling of astrocytes, which has been proposed to be a key factor of hepatic encephalopathy pathogenesis.<sup>3,10</sup> Both basal ganglia and occipital

white matter show a decrease of MTR in hepatic encephalopathy. Corresponding to <sup>1</sup>H-MR spectroscopy, this finding can be interpreted as a result of a general effect on the brain, but this finding may not be explained by an affect on the basal ganglia alone (see Figs 5-7).

The assessment of MTR only can hint at alterations in the brain-water content overall. To differentiate intra- and extracellular water content, DWI was performed. A generally accepted model of cytotoxic edema assumes that an increase of intracellular volume (ie, intracellular edema due to a shift of extracellular water) results in an impaired brownian molecular movement in the extracellular space and thus in a decrease of the ADC.<sup>23</sup> On the contrary, fluid leaving capillaries in vasogenic-interstitial edema enlarges extracellular space with an increase in ADC.

In the present study, ADC of the occipital white matter increased slightly with rising hepatic encephalopathy severity in the nonalcoholic patients. However, the ADC values of patients with overt hepatic encephalopathy only slightly exceeded those of the control group without reaching significance. This finding excludes demyelination or axonal loss, as found in trauma or multiple sclerosis, and massive cytotoxic edema, as found in acute stroke, as possible morphologic correlates of these findings. Demyelination, axonal loss, and cytotoxic edema would be expected to result in far more pronounced ADC disturbances.<sup>18,23,24</sup>

Changes in cerebral ADC are usually interpreted by using a 2-compartment model. Herein, the first compartment is the extracellular space with fast water molecule diffusion being the main contributor to the overall diffusivity. Water diffusion in the second compartment, the intracellular space, is slow and highly restricted, adding little to the overall diffusivity as assessed by the ADC. However, compartments of slow and fast diffusion may not depend only on the size of intra- and extracellular spaces, respectively, because factors different from those of compartments may influence ADC.<sup>25-28</sup> Minimal cellular edema with an increase of membrane permeability and increased intracellular diffusivity as well as changes in the vis-

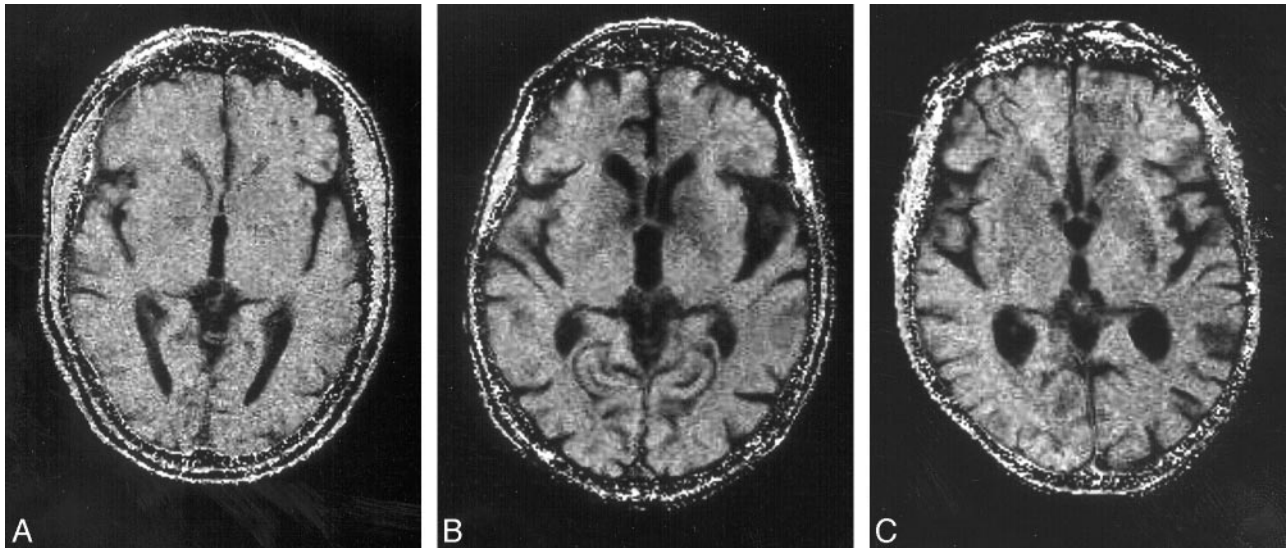


**Fig 6.** MTR map (width, 100%; center, 50%). *A*, Healthy volunteer (subject 8). *B*, Nonalcoholic patient with cirrhosis with HE 2 (subject 57). *C*, Alcoholic patient with cirrhosis with HE 2 (subject 59). MTR of volunteer (*A*): thalamus, 39.1%; pallidum, 36.4%; putamen, 37.3%; caudate, 37.5%. The following data refer to means of right and left side of the brain. MTR of nonalcoholic patients with cirrhosis (*B*): thalamus, 35.7%; pallidum, 27.0%; putamen, 31.1%; caudate, 27.7%. MTR of alcoholic patients with cirrhosis (*C*): thalamus, 34.8%; pallidum, 29.7%; putamen, 28.4%; caudate, 27.5%

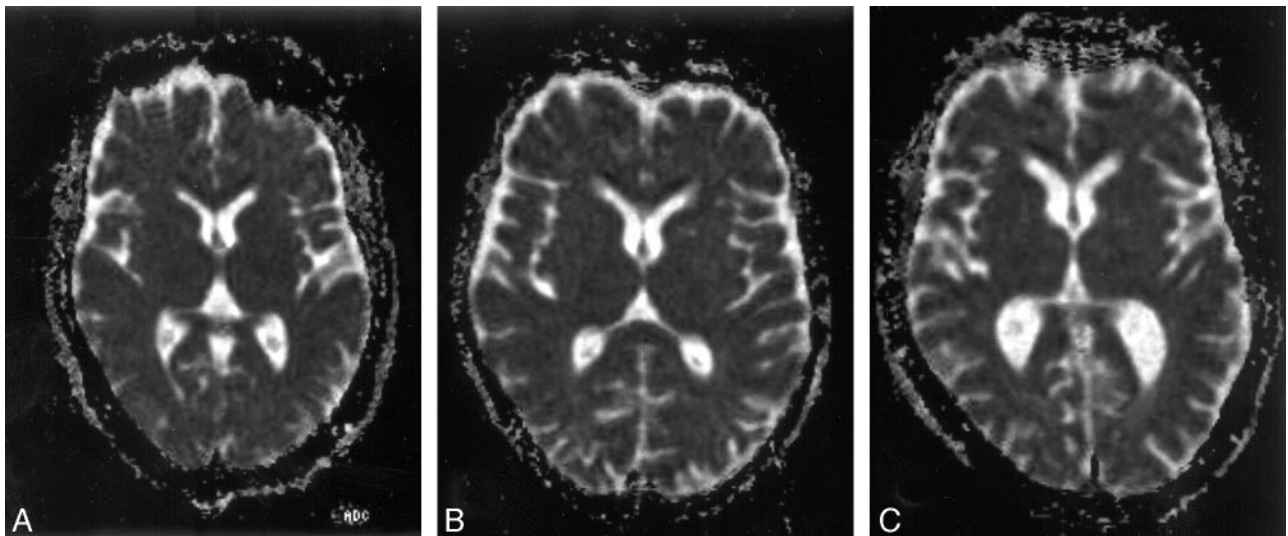


**Fig 7.** ADC map (width, 400%; center, 200%). *A*, Healthy volunteer (subject 14). *B*, Nonalcoholic patient with cirrhosis with HE 2 (subject 47). *C*, Alcoholic patient with cirrhosis and HE 2 (subject 50). ADC of volunteer (*A*): thalamus, 73.6; NAWM, 83.3. The following data refer to means of right and left side of the brain. ADC of nonalcoholic patients with cirrhosis (*B*): thalamus, 87.9; NAWM, 101.4. ADC of alcoholic patients with cirrhosis (*C*): thalamus, 80.6; NAWM, 108.

cosity of the cytoplasm are considered to be factors leading toward an increase in ADC.<sup>14</sup>

Electron microscopic studies on rat models of fulminant hepatic failure report both cytotoxic and vasogenic edema.<sup>29</sup> In this study, swelling of the perivascular astroglial foot process was the predominant finding, accompanied by a dilation of extracellular spaces in the cerebral cortex, pons, basal ganglia, and cerebellar cortex. A postmortem study on human brain material of 9 patients who died from hepatic coma reports comparable morphologic changes.<sup>30</sup> In this context, an increase in ADC may point to an extracellular component of low-grade cerebral edema in hepatic encephalopathy, whereas intracellular cytotoxic edema may be present at the same time and is best assessed by magnetization transfer imaging. However, because pathophysiology differs between fulminant hepatic failure and chronic hepatic encephalopathy, this theory awaits further study.

Moreover, the slight changes in intra- and extracellular water distribution and in water exchange between compartments that are possibly associated with hepatic encephalopathy may be too subtle to be detected sufficiently by DWI alone, because of its restricted spatial resolution.

In contrast to nonalcoholic patients, patients with liver cirrhosis of alcoholic etiology showed no correlation of MR findings with increasing hepatic encephalopathy severity, while exhibiting the same overall changes in <sup>1</sup>H-MR spectroscopy and magnetization transfer imaging as those of nonalcoholics. In view of an absent correlation between mIns/Cr and Glx/Cr ratios in the basal ganglia and in the occipital white matter, astrocyte edema with reactive mIns reduction alone may not fully explain the results of the present study.

One explanation for the discrepancy between the alcoholic and the nonalcoholic group may be microstructural lesions

resulting from chronic abuse of alcohol. A  $^1\text{H}$ -MR spectroscopy study on frontal lobe NAA loss in detoxified alcoholics ascribed neuronal loss or dysfunction to alcohol-induced oxidative stress.<sup>31</sup> These findings may in part explain the differences in  $^1\text{H}$ -MR spectroscopy results between alcoholics and nonalcoholics in the present study, because the NAA/Cr ratio in the basal ganglia was found to decrease with increasing Glx/Cr, as a possible hint to compromised neuronal integrity in the alcoholic group.

Alterations in DWI imaging in the brains of detoxified alcoholics have been reported.<sup>32</sup> Microstructural abnormalities (ie, disturbance of axonal integrity and changes in myelination and in water content) were considered to be the morphologic basis of these findings.

In alcoholics, neuronal membranes have ethanol-induced fluidity changes, which are subject to tolerance, as was first shown in animal models.<sup>33</sup> Membrane ethanol resistance is accompanied by an increased phospholipid turnover, as has been reported for rodents.<sup>34</sup> Altered membrane lipid composition, however, may result in changes of magnetization transfer effects.<sup>35</sup> Thus, alcohol-tolerant membranes in the brains of alcoholic patients with cirrhosis might exhibit a systematically different magnetization transfer ability than those of nonalcoholic patients with cirrhosis.

In the present study, duration of alcohol dependency, lifetime ethanol consumption, and time since the last drink were not recorded. Frontal lobe atrophy and cerebellar NAA and Cho decrease are frequent findings in alcoholics, NAA depletion and atrophy being reversible to some extent.<sup>36</sup> Because normalization occurred within the first 3 months of abstinence, assessment of duration of abstinence before imaging might add to the understanding of hepatic encephalopathy in detoxified alcoholic patients.

## Conclusion

White and gray matter MTR as well as white and gray matter Glx/Cr and mIns/Cr ratios correlated with the neuropsychologic status of nonalcoholic patients with cirrhosis.  $^1\text{H}$ -MR spectroscopy and magnetization transfer imaging are useful in assessing alterations attributed to changes in cerebral water content and distribution in different stages of hepatic encephalopathy.

No such correlation could be shown for alcoholic patients with cirrhosis, who exhibited similar overall alterations in magnetization transfer imaging and  $^1\text{H}$ -MR spectroscopy. This finding may hint at an interference of alcohol abuse with the pathophysiologic mechanisms perhaps due to direct toxic effects leading to a decrease in MTR and changes in  $^1\text{H}$ -MR spectroscopy in cirrhosis.

## References

- Häussinger D, Laubenberger J, vom Dahl S, et al. Proton magnetic resonance spectroscopy studies on human brain myo-inositol in hypo-osmolality and hepatic encephalopathy. *Gastroenterology* 1994;107:1475–80
- Kreis R, Ross BD. Cerebral metabolic disturbances in patients with subacute and chronic diabetes mellitus: detection with proton MR spectroscopy. *Radiology* 1992;184:123–30
- Laubenberger J, Häussinger D, Bayer S, et al. Proton magnetic resonance spectroscopy of the brain in symptomatic and asymptomatic patients with liver cirrhosis. *Gastroenterology* 1997;112:1610–16
- Cordoba J, Alonso J, Rovira A, et al. The development of low-grade cerebral edema in cirrhosis is supported by the evolution of (1)H-magnetic resonance abnormalities after liver transplantation. *J Hepatol* 2001;35:598–604
- Geissler A, Lock G, Frund R, et al. Cerebral abnormalities in patients with

- cirrhosis detected by proton magnetic resonance spectroscopy and magnetic resonance imaging. *Hepatology* 1997;25:48–54
- Ross BD, Jacobson S, Villamil F, et al. Subclinical hepatic encephalopathy: proton MR spectroscopic abnormalities. *Radiology* 1994;193:457–63
- Lee JH, Seo DW, Lee YS, et al. Proton magnetic resonance spectroscopy (1H-MRS) findings for the brain in patients with liver cirrhosis reflect the hepatic functional reserve. *Am J Gastroenterol* 1999;94:2206–13
- Butterworth RF. Pathogenesis of hepatic encephalopathy: new insights from neuroimaging and molecular studies. *J Hepatol* 2003;39:278–85
- Cordoba J, Sanpedro F, Alonso J, et al. 1H magnetic resonance in the study of hepatic encephalopathy in humans. *Metab Brain Dis* 2002;17:415–29
- Häussinger D, Kircheis G, Fischer R, et al. Hepatic encephalopathy in chronic liver disease: a clinical manifestation of astrocyte swelling and low-grade cerebral edema? *J Hepatol* 2000;32:1035–38
- Rovira A, Grive E, Pedraza S, et al. Magnetization transfer ratio values and proton MR spectroscopy of normal-appearing cerebral white matter in patients with liver cirrhosis. *AJNR Am J Neuroradiol* 2001;22:1137–42
- Iwasa M, Kinoshita Y, Nakatsuka A, et al. Magnetization transfer contrast of various regions of the brain in liver cirrhosis. *AJNR Am J Neuroradiol* 1999;20:652–54
- Rovira A, Cordoba J, Sanpedro F, et al. Normalization of T2 signal abnormalities in hemispheric white matter with liver transplant. *Neurology* 2002;59:335–41
- Lodi R, Tonon C, Straciarri A, et al. Diffusion MRI shows increased water apparent diffusion coefficient in the brains of cirrhotics. *Neurology* 2004;62:762–66
- Pugh RN, Murray-Lyon IM, Dawson JL, et al. Transection of the oesophagus for bleeding oesophageal varices. *Br J Surg* 1973;60:646–49
- Schuhfried G. *Wiener Test System (WINWTS)*. Schuhfried: Mödling, Austria; 1999
- Sinson G, Bagley LJ, Cecil KM, et al. Magnetization transfer imaging and proton MR spectroscopy in the evaluation of axonal injury: correlation with clinical outcome after traumatic brain injury. *AJNR Am J Neuroradiol* 2001;22:143–51
- Ge Y, Grossman RI, Udupa JK, et al. Magnetization transfer ratio histogram analysis of gray matter in relapsing-remitting multiple sclerosis. *AJNR Am J Neuroradiol* 2001;22:470–75
- Provencher SW. Automatic quantitation of localized in vivo 1H spectra with LCModel. *NMR Biomed* 2001;14:260–64
- Filippi M, Campi A, Dousset V, et al. A magnetization transfer imaging study of normal-appearing white matter in multiple sclerosis. *Neurology* 1995;45(3 Pt 1):478–82
- Hahnel S, Munkel K, Jansen O, et al. Magnetization transfer measurements in normal-appearing cerebral white matter in patients with chronic obstructive hydrocephalus. *J Comput Assist Tomogr* 1999;23:516–20
- Brochet B, Dousset V. Pathological correlates of magnetization transfer imaging abnormalities in animal models and humans with multiple sclerosis. *Neurology* 1999;53(5 suppl 3):S12–17
- Lansberg MG, Thijs VN, O'Brien MW, et al. Evolution of apparent diffusion coefficient, diffusion-weighted, and T2-weighted signal intensity of acute stroke. *AJNR Am J Neuroradiol* 2001;22:637–44
- Gass A, Niendorf T, Hirsch JG. Acute and chronic changes of the apparent diffusion coefficient in neurological disorders: biophysical mechanisms and possible underlying histopathology. *J Neurol Sci* 2001;186(suppl 1):S15–23
- Niendorf T, Dijkhuizen RM, Norris DG, et al. Biexponential diffusion attenuation in various states of brain tissue: implications for diffusion-weighted imaging. *Magn Reson Med* 1996;36:847–57
- Assaf Y, Cohen Y. Detection of different water populations in brain tissue using 2H single- and double-quantum-filtered diffusion NMR spectroscopy. *J Magn Reson B* 1996;112:151–59
- Mulkern RV, Gudbjartsson H, Westin CF, et al. Multi-component apparent diffusion coefficients in human brain. *NMR Biomed* 1999;12:51–62
- Chin CL, Wehrli FW, Hwang SN, et al. Biexponential diffusion attenuation in the rat spinal cord: computer simulations based on anatomic images of axonal architecture. *Magn Reson Med* 2002;47:455–60
- Kato M, Sugihara J, Nakamura T, et al. Electron microscopic study of the blood-brain barrier in rats with brain edema and encephalopathy due to acute hepatic failure. *Gastroenterol Jpn* 1989;24:135–42
- Kato M, Hughes RD, Keays RT, et al. Electron microscopic study of brain capillaries in cerebral edema from fulminant hepatic failure. *Hepatology* 1992;15:1060–66
- Schweinsburg BC, Taylor MJ, Alhassoon OM, et al. Chemical pathology in brain white matter of recently detoxified alcoholics: a 1H magnetic resonance spectroscopy investigation of alcohol-associated frontal lobe injury. *Alcohol Clin Exp Res* 2001;25:924–34
- Pfefferbaum A, Sullivan EV. Microstructural but not macrostructural disruption of white matter in women with chronic alcoholism. *Neuroimage* 2002;15:708–18
- Chin JH, Goldstein DB. Drug tolerance in biomembranes: a spin label study of the effects of ethanol. *Science* 1977;196:684–85
- Lee NM, Friedman HJ, Loh HH. Effect of acute and chronic ethanol treatment on rat brain phospholipid turnover. *Biochem Pharmacol* 1980;29:2815–18
- Fralix TA, Ceckler TL, Wolff SD, et al. Lipid bilayer and water proton magnetization transfer: effect of cholesterol. *Magn Reson Med* 1991;18:214–23
- Parks MH, Dawant BM, Riddle WR, et al. Longitudinal brain metabolic characterization of chronic alcoholics with proton magnetic resonance spectroscopy. *Alcohol Clin Exp Res* 2002;26:1368–80